Electronic Supplementary Material (ESI) for RSC Advances.
This journal is © The Royal Society of Chemistry 2014

Electronic Supplementary Information

Growth of Hexagonal Phase Sodium Rare Earth Tetrafluorides Induced by Heterogeneous Cubic Phase Core

Dan Zhao, Huan Chen, Kezhi Zheng, Xiaohong Chuai, Fangda Yu, Hui Li, Changfeng Wu, Guanshi Qin, Weihua Di and Weiping Qin*

State Key Laboratory on Integrated Optoelectronics, College of Electronic Science and Engineering, Jilin University 2699 Qianjin Street, Changchun, 130012 (P. R. China).

Contents

1. Experimental

1.1 Materials used for synthesis

The rare earth chlorate, including lutetium chlorate ($LuCl_3$), yttrium chlorate YCl_3, ytterbium chlorate ($YbCl_3$), erbium chlorate ($ErCl_3$) were obtained from Sandong Yutai Rare Earth Technology Co., Ltd. China (all with purity > 99.9%). Sodium chlorate (NaCl, AR), sodium fluoride (NaF, AR), hydrochloric acid (HCl, 37 wt %) and ethylene glycol (EG, AR) were bought form Shanghai Shabo Chemical Technology Co., Ltd. China. Polyvinylpyrrolidone K-30 (PVP, 58000 g/mol) was obtained from Aldrich. All chemicals were used as received and without further purification.

1.2 Synthesis procedures of core/shell hetero structures

1.2.1 Synthesis of the cubic $NaREF_4$ core

Metal chlorate ($RECl_3$, NaCl) stock solutions were prepared by dissolving the corresponding metal chlorate in EG. Polyvinylpyrrolidone K-30 (PVP, 0.5 g) was dissolved in EG (10 mL) to form a transparent solution. For synthesis of α-$NaLuF_4$ nanocrystals, $LuCl_3$ (1 mmol) and NaCl (1 mL, 1 mmol) EG solutions were subsequently added into PVP solution under strong stirring to form a solution. KF (6 mmol) was also dissolved in EG and added dropwise into above solution. The mixture was stirred for 2 hours and transferred to a polytetrafluoroethylene autoclave, and then heated at 180 °C for 24 hours. The autoclave was cooled to room temperature. The resulting product was dispersed in 10 mL EG as core for further synthesis. The synthesis process of the α-$NaYF_4$ nanocrystals was similar, just using YCl_3 solution as precursor.

1.2.2 Synthesis of the core/shell hybrid nanocrystals

For synthesis of α-$NaLuF_4$/β-$NaYF_4$ hybrid nanocrystals (HNCs), PVP (0.5 g) was dissolved in the α-$NaLuF_4$ core solution. Then YCl_3 (1 mmol), $YbCl_3$ (0.18 mmol), $ErCl_3$ (0.02 mmol) and NaCl (5 mmol) EG solutions were added respectively under stirring. KF (6 mmol) was dissolved in EG (7 mL), and was subsequently added dropwise into above mixture. After stirring for 1 hour,

the solution was then transferred into a polytetrafluoroethylene autoclave and reacted at 180 °C for 24 hours. The final product was obtained by centrifugation and washed with ethanol for several times. Half of the final product was dried in vacuum oven at 80 °C for XRD, TEM detection. The other half counterpart was redispersed in water to get the clear solution. To obtain α-$NaYF_4$/β-$NaLuF_4$ HNCs, the synthesis process was similar. The α-$NaLuF_4$ was used as core and the $LuCl_3$ EG solution was used as precursor.

1.2.3 Synthesis of two sets of α-$NaREF_4$/β-$NaRE'F_4$ hybrid nanocrystals as control experiments

A set of α-$NaLuF_4$/β-$NaYF_4$ HNCs was prepared at 180 °C for 6, 12, 24 hours, respectively. The cubic $NaLuF_4$ cores were the same batch of product which was used in the above heterogeneous growth process. Other growth conditions were identical except the growth time. The synthesis process of the set of α-$NaYF_4$/β-$NaLuF_4$ HNCs was similar. The α-$NaYF_4$ was used as core and the $LuCl_3$ was used as precursor.

1.2.4 Two sets of control experiments using homogenous cubic phase $NaREF_4$ cores

The synthesis process was similar with HNCs. The same batch of cubic $NaYF_4$ or $NaLuF_4$ cores were used in the above heterogeneous growth process. With the same reaction conditions as those for the heterogeneous growth process, the core nanocrystals were introduced into the relative solutions containing the $NaYF_4$ or $NaLuF_4$ precursors to achieve homogenous core/shell structures.

2. Characterization

XRD analysis was carried out with a powder diffractometer (Model Rigaku RU-200b), using Ni-filtered Cu Kα radiation (λ= 1.5406 Å) with 200 mA current and 50 kV voltage across the tube to generate powerful X-ray. The XRD measurement was performed at a scan rate of $18°min^{-1}$ and step size of 0.02°. Transmission electron microscopy (TEM) and high-resolution transmission electron microscopy (HRTEM) were recorded on an FEI Tenai F-20 microscope with a field emission gun operating at 200 kV. Images were acquired digitally by a CCD camera. The local

elemental mapping and elemental compositions were determined by energy-dispersive X-ray spectrometry (EDX) under the HR-TEM mode. The upconversion (UC) emission spectra were recorded by a fluorescence spectrometer (Hitachi F-4500) equipped with a 980-nm diode laser. The UC luminescent photos of the aqueous solution were taken by a Nikon digital camera (D300s). The digital photographs were taken using identical camera settings and same pumping power. All the measurements were performed at room temperature.

3. Supplementary Figures and Discussion

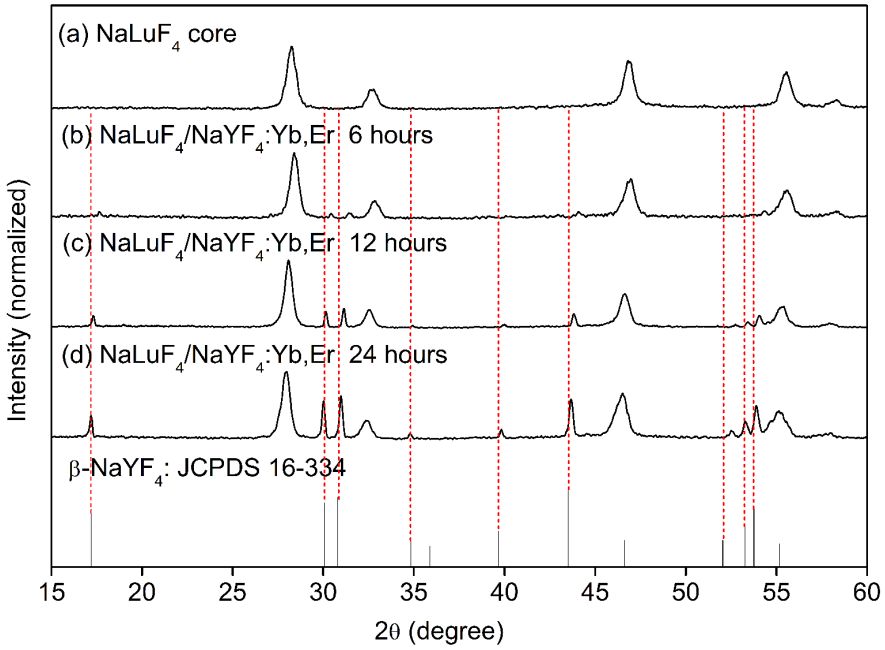

Fig. S1 XRD patterns (a) α-$NaLuF_4$ cores; (b-d) α-$NaLuF_4$/β-$NaYF_4$ HNCs, the shell growth time is increased, (b) 6 hours, (c) 12 hours, (d) 24 hours; (bottom) standard XRD data of β-$NaYF_4$ crystal (JCPDS file number 16-0334).

The XRD patterns of core can be indexed as pure cubic phase $NaLuF_4$ crystal.[1] After the α-$NaLuF_4$ core was reacted with the $NaYF_4$ precursors for 6 hrs, the diffraction peaks corresponding to hexagonal phase counterpart were appeared in the XRD patterns. A gradual increase in diffraction peak intensities for the hexagonal phase counterpart is observed as increased reaction time. It indicates that the fraction of hexagonal phase counterparts in the shells is gradually increased. Compared to the pure β-$NaYF_4$, slight diffraction peak shifts of hexagonal phase are observed in the

XRD patterns of 6-hour and 12-hour samples. It is an powerful evidence for the formation of Y-Lu hetero interface in a single HNC. The peak shifts become smaller and smaller with increasing the reaction time. For the 24-hour samples, the profile of the XRD pattern for the hexagonal-phase counterparts nearly match with the standard β-$NaYF_4$ crystal. This evolution of diffraction peak shifts indicates that as the shell grows up, the target β-$NaYF_4$ gradually becomes dominated in the shell and the fraction of hetero interface in the whole HNCs becomes smaller.

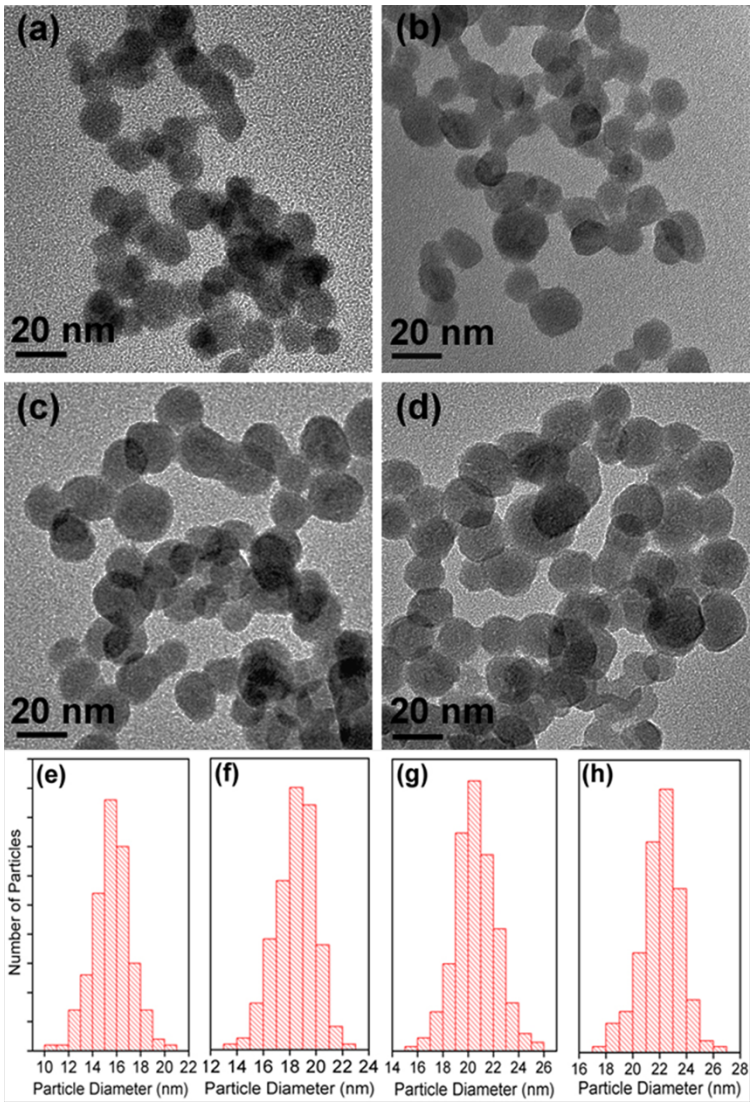

Fig. S2 TEM images and size distribution. (a) and (e) α-$NaLuF_4$ cores; (b-d) and (f-h) α-$NaLuF_4$/β-$NaYF_4$ HNCs, shell growth time is increased, (b) and (f) 6 hours; (c) and (g) 12 hours; (d) and (h) 24 hours.

All samples are nearly spherical. The size of α-$NaLuF_4$ core is about 15 nm. A gradual increase of size from 18 nm to 22 nm is observed in HNCs as the shell growth time is increased.

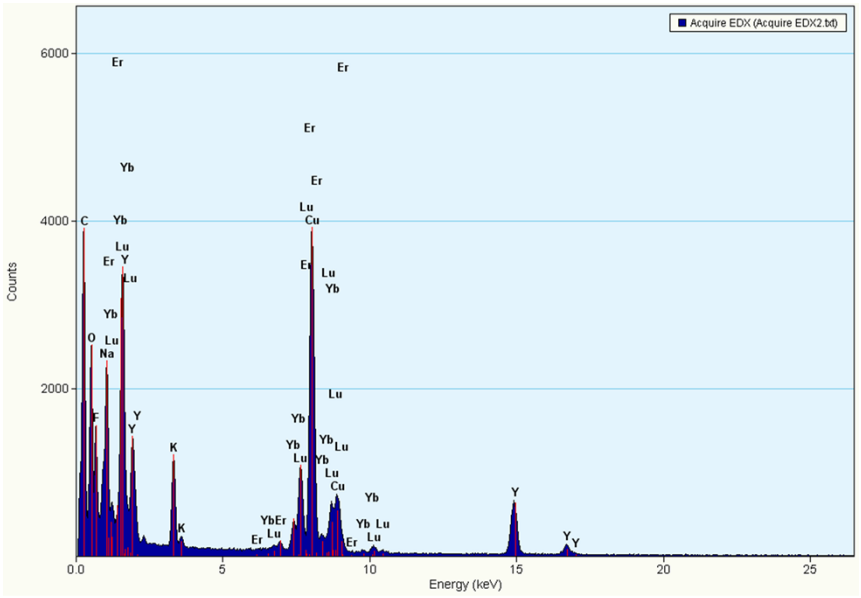

Fig. S3 EDX analysis of elemental composition of α-$NaLuF_4$/β-$NaYF_4$ HNCs.

Both the Lu, Y, Yb and Er elements are observe in the curve, which reveals that a $NaYF_4$:Yb,Er layer has been grown on the $NaLuF_4$ cores.

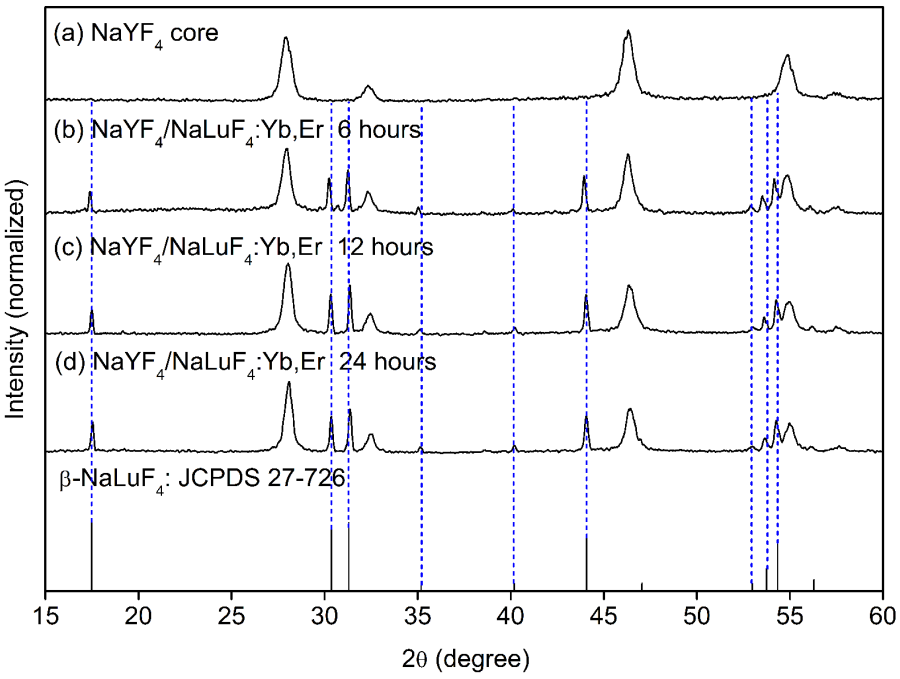

Fig. S4. XRD patterns (a) α-$NaYF_4$ cores; (b-d) α-$NaYF_4$/β-$NaLuF_4$ HNCs, the shell growth time is increased, (b) 6 hours, (c) 12 hours, (d) 24 hours; (bottom) standard XRD data of β-$NaLuF_4$ crystal (JCPDS file number 27-726).

After the α-$NaYF_4$ core was reacted with the $NaLuF_4$ precursors for 6 hours, the diffraction peaks corresponding to hexagonal phase counterpart were appeared in the XRD patterns. We also

observe a gradual increase in diffraction peak intensities for the hexagonal phase counterpart is observed as a function of increased reaction time. However, such increase is small. Compared to the pure β-$NaLuF_4$, slight diffraction peak shifts of hexagonal phase are also observed in the XRD patterns of 6-hour and 12-hour samples. These peak shifts are consistent with the formation of the hetero interface. For the 24-hour samples, the profile of the XRD pattern for the hexagonal phase counterparts nearly match with the standard β-$NaLuF_4$ crystal. This evolution of diffraction peak shifts is also an evidence for the growth of hexagonal phase $NaLuF_4$.

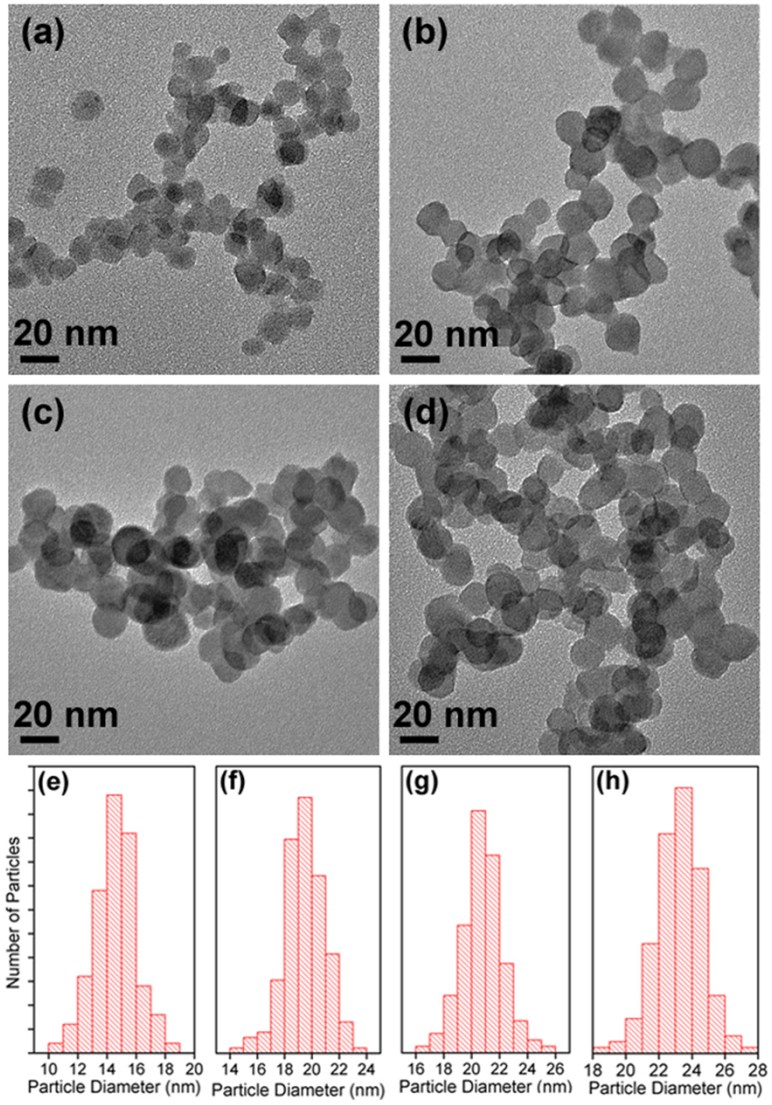

Fig. S5 TEM images and size distribution. (a) and (e) α-$NaYF_4$ cores; (b-d) and (f-h) α-$NaYF_4$/β-$NaLuF_4$ HNCs, shell growth time is increased, (b) and (f) 6 hours; (c) and (g) 12 hours; (d) and (h) 24 hours.

All samples are nearly spherical. The size of α-$NaYF_4$ core is about 14 nm. A gradual increase of size from 18 nm to 22 nm is observed in HNCs as the shell growth time is increased.

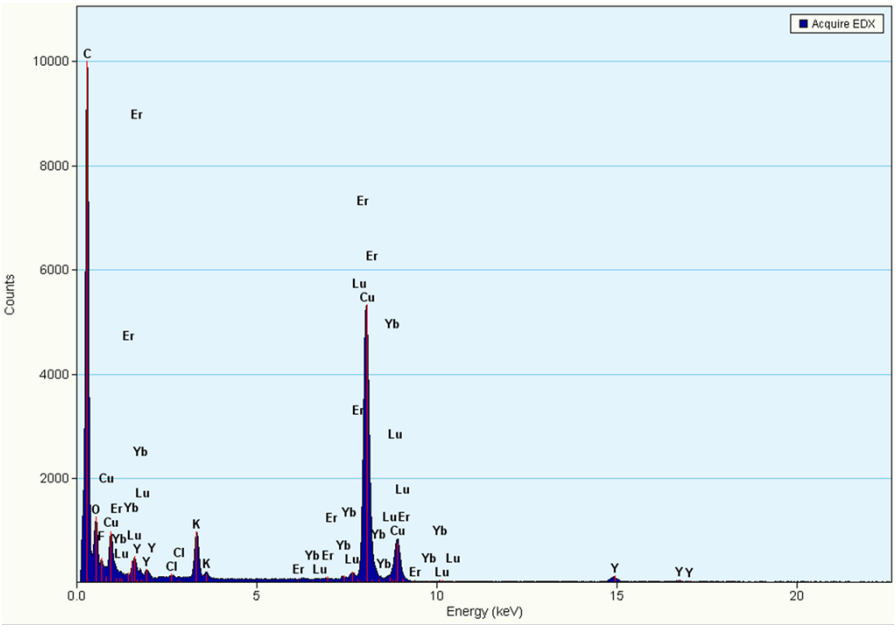

Fig. S6 EDX analysis of elemental composition of α-$NaYF_4$/β-$NaLuF_4$ HNCs.

The Y, Lu, Yb and Er elements emerging in the curve reveals that a $NaLuF_4$:Yb,Er layer has been grown on the $NaYF_4$ cores.

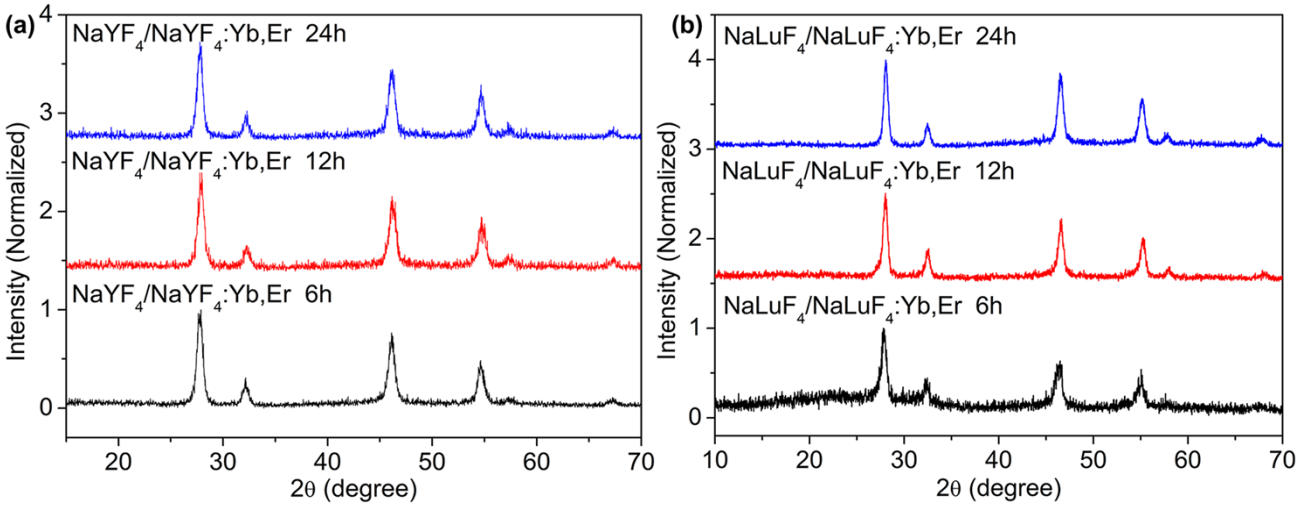

Fig. S7 Two sets of control experiments using homogenous cores, (a) XRD patterns of α-$NaYF_4$/$NaYF_4$ nanoparticles, shell growth time is 6, 12 and 24 hours; (b) XRD patterns of α-$NaLuF_4$/$NaLuF_4$ nanoparticles, reaction time is 6, 12 and 24 hours.

In both two sets of control experiments, the core nanocrystals were introduced into the relative solutions containing the $NaYF_4$ or $NaLuF_4$ precursors to achieve homogenous core/shell structures. With the same reaction conditions as those for the heterogeneous growth process, there were no obvious hexagonal phase diffraction peaks observed in the XRD patterns.

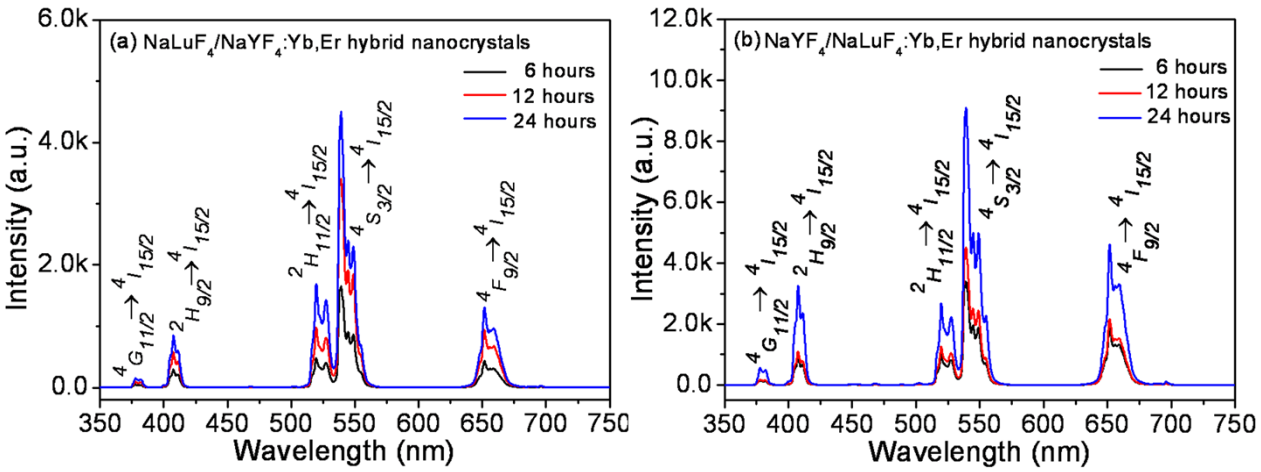

Fig. S8 UC emission spectra of the two sets of HNCs under 980-nm excitation (excitation power is 20 mW). The shell growth time is increased form 6 hours to 24 hours. (a) α-$NaLuF_4$/β-$NaYF_4$:Yb,Er HNCs; (b) α-$NaYF_4$/β-$NaLuF_4$:Yb,Er HNCs.

The sensitizer inos, Yb^{3+} (20 mol%), and luminescent center ions, Er^{3+} (3 mol%), were codoped in the hexagonal phase shells. The UC emission intensity of each sets of HNCs was gradually increased with the shell growth time. Under the same pumping power, the UC emission intensity of the α-$NaYF_4$/β-$NaLuF_4$ HNCs is about 2 times stronger than α-$NaLuF_4$/β-$NaYF_4$ HNCs.

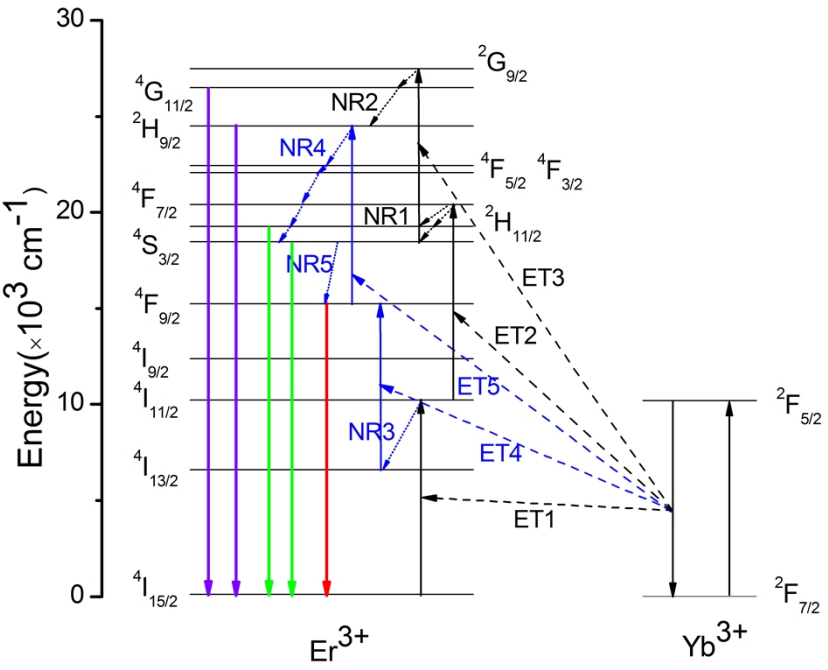

Fig. S9. Energy level diagrams of Yb^{3+} and Er^{3+} ions, and possible UC processes.

In a Yb^{3+} and Er^{3+} codoped system, emission levels of Er^{3+} ions can be populated by the energy transfer (ET) from excited Yb^{3+} ions and nonradiative relaxation (NR) from higher energy levels of Er^{3+} ions. The UC luminescence of Er^{3+} ions is obtained by the radiative transition from corresponding energy levels. In our previous work, we had demonstrated there were two different population routes of Er^{3+} ions in hexagonal phase crystals due to the pumping power of 980 nm laser.[2] For the population of $^4G_{9/2}$ and $^2H_{9/2}$, the possible route 1 is $^4I_{15/2} \xrightarrow{ET1} {}^4I_{11/2} \xrightarrow{ET2} {}^4F_{7/2} \xrightarrow{NR1} {}^2H_{11/2}$, $^4S_{3/2} \xrightarrow{ET3} {}^2G_{9/2} \xrightarrow{NR2} {}^4G_{11/2}$, $^2H_{9/2}$. The route 2 is $^4I_{15/2} \xrightarrow{ET1} {}^4I_{11/2} \xrightarrow{NR3} {}^4I_{13/2} \xrightarrow{ET4} {}^4F_{9/2} \xrightarrow{ET5} {}^2H_{9/2} \xrightarrow{NR4} {}^2H_{11/2}$, $^4S_{3/2} \xrightarrow{ET3} {}^2G_{9/2} \xrightarrow{NR2} {}^4G_{11/2}$, $^2H_{9/2}$. In this work, the power density is lower than 20W/cm^2. Therefore, route 1 is the dominant way to populate the $^4S_{3/2}$. In the UC emission spectra (Fig. S8), the emission peaks centered at 370 and 408 nm correspond to the $^4G_{11/2} \rightarrow {}^4I_{15/2}$ and $^2H_{9/2} \rightarrow {}^4I_{15/2}$ transitions, respectively. The emissions in the range from 520 nm to 570 nm are from $^2H_{11/2} \rightarrow {}^4I_{15/2}$ and $^4S_{3/2} \rightarrow {}^4I_{15/2}$ transitions. The red emission centered at 657 nm is from the $^4F_{9/2} \rightarrow {}^4I_{15/2}$ transition.

4. Table for Pumping power threshold

Table S1. Pumping power threshold for UC emission of α-$NaLuF_4$/β-$NaYF_4$:Yb,Er and α-$NaYF_4$/β-$NaLuF_4$:Yb,Er HNCs (for 24-hour samples). The relative pumping threshold for one UC emission was defined as the pump power density that the emission peak just appears in the measured UC spectrum with increasing the pump power.[3]

Emission wavelength (nm)	Threshold power density for α-$NaLuF_4$/β-$NaYF_4$:Yb,Er hybrid nanoparticles (mW/cm^2)	Threshold power density for α-$NaYF_4$/β-$NaLuF_4$:Yb,Er hybrid nanoparticles (mW/cm^2)
409 nm	195.8	146.0
542 nm	6.6	1.2
650 nm	18.0	2.6

References

1. (a) J. Lin, C. X. Li, J. Yang, P. P. Yang, X. M. Zhang and H. Z. Lian, *Cryst Growth Des*, 2008, **8**, 923. (b) F. Shi, J. S. Wang, X. S. Zhai, D. Zhao and W. P. Qin, *Crystengcomm*, 2011, **13**, 3782.
2. K. Zheng, L. Wang, D. Zhang, D. Zhao, and W. Qin, *Opt. Express*, 2010, **18**, 2934.
3. N. Liu, W. P. Qin, G. S. Qin, T. Jiang and D. Zhao, *Chem Commun*, 2011, **47**, 7671.